



Title	NUMERICAL ANALYSIS OF INFLUENCING FACTORS ON CORROSION-INDUCED CONCRETE CRACKING WITH RBSM
Author(s)	QIAO, D.; NAKAMURA, H.; KUNIEDA, M.; UEDA, N.
Citation	Proceedings of the Thirteenth East Asia-Pacific Conference on Structural Engineering and Construction (EASEC-13), September 11-13, 2013, Sapporo, Japan, C-6-5., C-6-5
Issue Date	2013-09-11
Doc URL	http://hdl.handle.net/2115/54298
Type	proceedings
Note	The Thirteenth East Asia-Pacific Conference on Structural Engineering and Construction (EASEC-13), September 11-13, 2013, Sapporo, Japan.
File Information	easec13-C-6-5.pdf



[Instructions for use](#)

NUMERICAL ANALYSIS OF INFLUENCING FACTORS ON CORROSION-INDUCED CONCRETE CRACKING WITH RBSM

D. QIAO^{1*}, H. NAKAMURA¹, M. KUNIEDA¹ and N. UEDA¹

¹ *Department of Civil Engineering, Nagoya University, Japan*

ABSTRACT

This study presented a discussion based on parameter analysis about effects of mechanical properties of concrete cover, specimen width and cover thickness on cracking process, in which Rigid Body Spring Method with corrosion expansion model was used. The numerical results show that for normal concrete specimen, thicker cover can extend the time until surface crack initiation and wider specimen will result in smaller surface crack width. It is also found that surface crack initiation is controlled by tensile strength while increasing fracture energy can retard propagation of surface crack width. Moreover higher fracture energy for wide specimen will cause internal cracks develop diagonally toward surface rather than sides of concrete and lead to a smaller spalling volume finally. Therefore it can be verified that ductile materials having high fracture energy is available to control cracking damage of concrete due to rebar corrosion.

Keywords: Corrosion, Crack Propagation, Fracture Energy, Spalling Volume

1. INTRODUCTION

Durability of reinforced concrete structures is affected by rebar corrosion when exposed to aggressive environment, such as chloride and acid attack. Corrosion products occupy larger volume than original rebar, impose expansion pressure on surrounding concrete and lead to concrete cracking. At present a number of researches (Alonso et al. 1998; Xiao et al. 2011) were presented to study influencing factors on cracking behavior. However, the dominant factors in crack initiation and propagation are not clear as many factors have impacts on cracking behavior, such as material properties of concrete cover and geometrical properties of specimen. Moreover, study of effects on corrosion-induced cracking considering material properties will benefit repair work in terms of determining appropriate repair materials. On the other hand, analytical method developed from observations found in corrosion experiment is very convenient to study various effects on cracking behavior, which are difficult to investigate through experiment. Hence analytical method was used in this study.

This study analyzes the effects of mechanical and geometrical properties of concrete specimen on corrosion-induced cracking, including tensile strength, fracture energy, cover thickness and

* Corresponding author and presenter: Email: qiao.di@i.mbox.nagoya-u.ac.jp

specimen width, in which Rigid Body Spring Method combined with corrosion expansion model (Tran et al. 2011) is used.

2. ANALYSIS OUTLINE

2.1. RBSM Model

Rigid Body Spring Method is a kind of discrete approaches, which is easy to simulate concrete cracking process. This method represents a continuum material as an assemblage of rigid particle elements interconnected by zero springs along their boundaries (Figure 1). The elements are randomly generated by Voronoi Diagram. In this study, three dimensional RBSM was applied in parameter analysis (Yamamoto et al. 2008).

Figure 2 shows material models of concrete used in analysis. Tensile and compressive models are introduced into normal springs, in which f_t represents tensile strength, G_F tensile fracture energy, h distance between centers of Voronoi elements, f_c' compressive strength, G_{FC} compressive fracture energy and E Young modulus. Shear model is introduced into shear springs. Also, shear reduction model with crack width is applied and shear strength is defined by Mohr-Coulomb criterion.

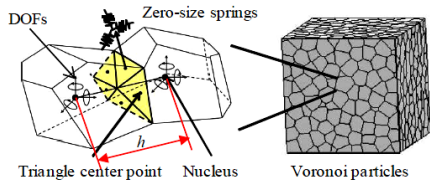


Figure 1: 3D RBSM model

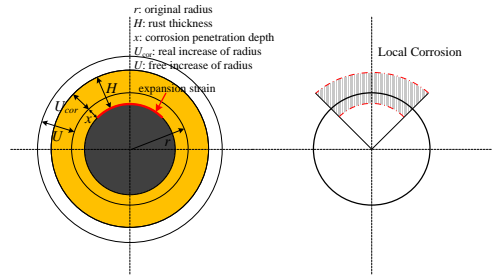


Figure 3 Corrosion expansion model

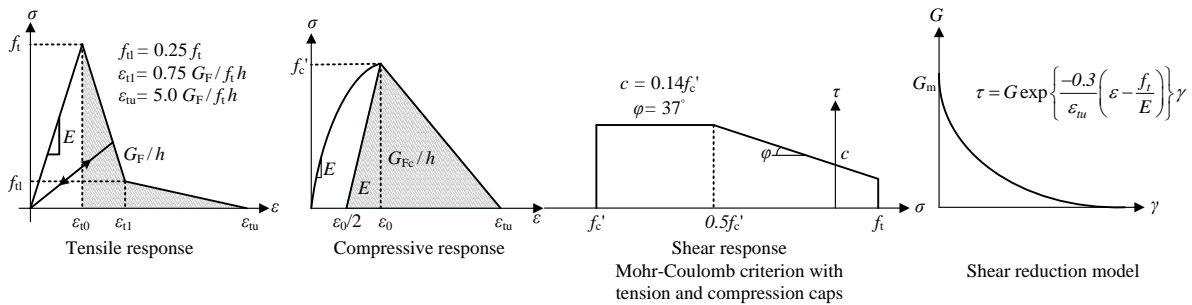


Figure 2 Concrete materials model

2.2. Corrosion Expansion Model

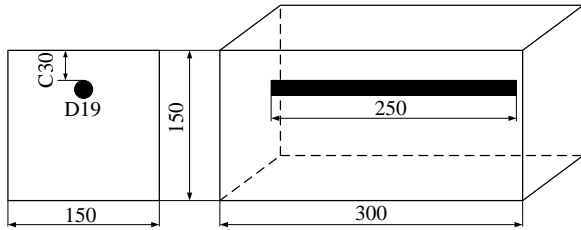
Expansion of corrosion products caused by rebar corrosion inside concrete was modeled by internal expansion pressure, which took local corrosion into account as shown in Figure 3. In this method, expansion pressure was simulated with increment of initial strain applied on the boundary between corrosion product layer and rebar layer, which was calculated by equation (1):

$$\Delta\sigma_{cor} = E_r (\Delta\varepsilon - \Delta\varepsilon_0) = E_r \left(\frac{\Delta U_{cor}}{H} - \frac{\Delta U}{H} \right) \quad (1)$$

Where E_r is elastic modulus of rust, ΔU_{cor} increment of real increase of rebar radius confined by surrounding concrete, ΔU free increase of rebar radius and H thickness of corrosion product layer. During simulation, increment of initial strain was only applied over one-quarter of the model to consider local corrosion. This model combined with RBSM method is appropriate to evaluate corrosion-induced cracking behavior of concrete cover and agrees well with accelerated corrosion test result, such as surface crack width development and internal crack patterns (Tran et al. 2011).

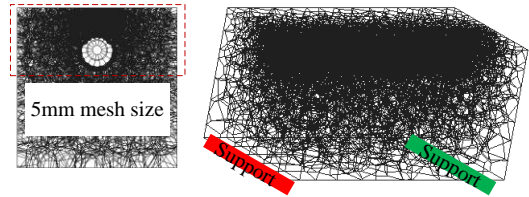
2.3. Specimen

Single-rebar specimens with a rebar diameter of 19mm were simulated in this study. Established specimens have a height of 150mm and a length of 300mm. The specimen width is changed to 150mm, 300mm and 600mm respectively and cover thickness is changed from 10mm to 30mm. Figure 4 shows the basic specimen, which was also tested by accelerated corrosion test (Tran et al. 2011). During test, surface crack width and internal crack pattern were observed. RBSM model for these specimens were created as shown in Figure 5. It is noted that specimen length was reduced to 100mm for specimens wider than 150mm to reduce numbers of elements in calculation.



a) Section view b) Side view

Figure 4: Specimen dimensions



a) Specimen section b) 3D Voronoi particles

Figure 5: RBSM model of specimen

2.4. Analytical Parameter

Two groups of mechanical properties were adopted in the simulation work for analyzing effects of mechanical properties of concrete cover on cracking behavior. In the first group, tensile strength has a range of 2.22 to 6.43MPa while fracture energy keeps the same as 84.3N/m. In the other group,

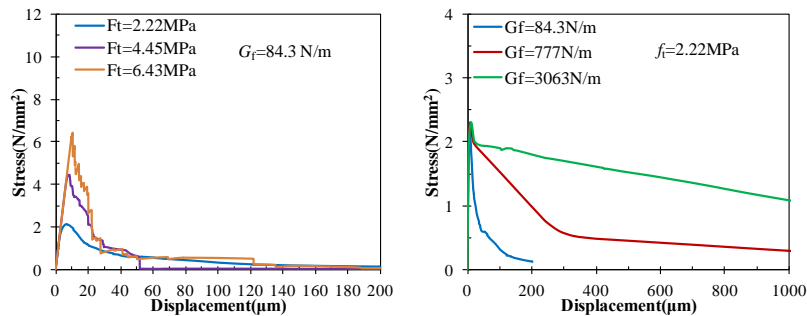


Figure 6: Stress-displacement relationship of analytical specimens

tensile strength keeps as 2.22MPa while fracture energy increases from 84.3 to 3063N/m. Deformation versus stress relationship based on the two groups of mechanical properties are shown separately in Figure 6. These results were obtained by tension test simulation based on the same mesh size as following analysis of influencing factors on corrosion-induced cracking.

3. CRACK PROPAGATION BEHAVIOR FOR NORMAL MATREIAL PROPETIES

Cracking behavior of normal concrete specimen with a tensile strength of 2.22MPa and fracture energy of 84.3N/m is significantly influenced by the geometrical properties. Figure 7 presents surface crack development of normal concrete specimens having a width of 150mm and 600mm separately, which also varies in cover thicknesses. It is shown that surface crack initiation will be delayed by an increase of cover thickness. On the other hand, after crack initiation, a larger crack width will be caused by thicker concrete cover due to stronger bending effects.

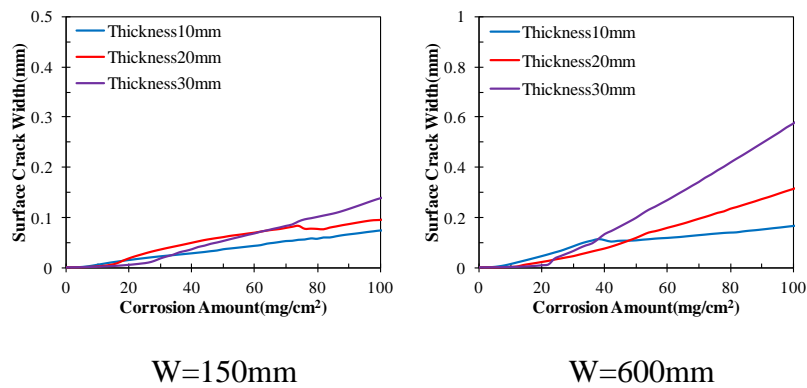


Figure 7: Surface crack development for different cover thicknesses

Figure 8 shows surface crack propagation versus corrosion amount for different specimen widths. It is observed that corrosion amount corresponding to surface crack appearance keeps the same for different specimen widths. However a smaller specimen width will result in a larger crack width. Narrow concrete cover leads to a bigger surface uplift due to the limited boundary size as shown in Figure 9 and consequently causes a larger surface crack width.

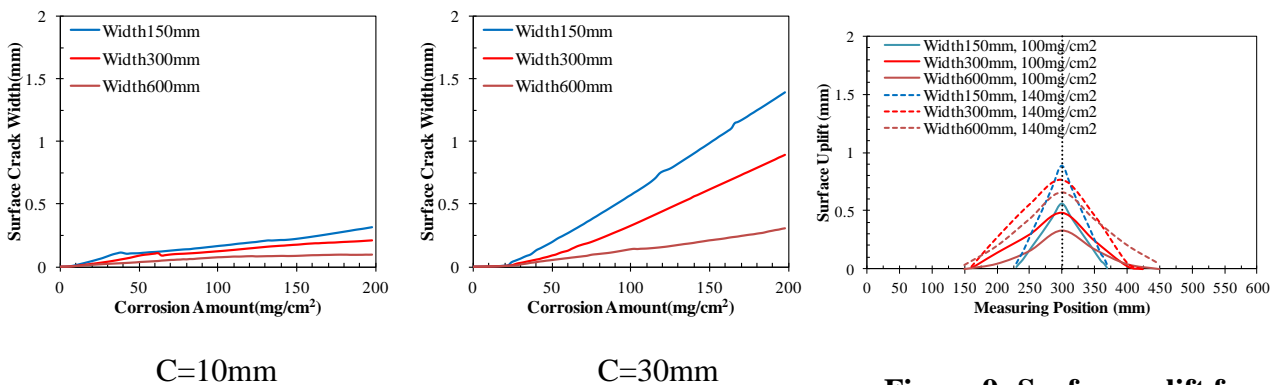


Figure 9: Surface uplift for different specimen width

Figure 8: Surface crack development for different specimen width

Figure 10 compares internal crack pattern of normal concrete with different geometrical properties under a corrosion amount of $100\text{mg}/\text{cm}^2$, in which red areas represent cracks with a width of 0.1mm and over. When cover thickness of concrete specimens is 10mm , lateral cracks propagate toward to concrete surface instead of sides of concrete specimen, which is different from the case of bigger cover thickness. It is proposed that if the ratio of cover thickness to rebar diameter less than 1, internal cracks develop toward concrete surface diagonally. Comparatively, internal crack propagate respectively to sides and surface in the shortest path when this ratio larger than 1 (Tsutsumi et al. 1996). It is mentioned above that surface crack width for specimens with a cover thickness of 10mm is smaller as shown in Figure 8 and surface cracking behavior is different from thicker specimen as shown in Figure 7. The reason can be attributed to the differences of internal crack patterns. It is noted that it is easy to incur cover spalling with a small volume in the case of 10mm cover thickness. However in the case of thicker cover, spalling volume will become bigger due to propagation of lateral cracks inside concrete, if cover spalling behavior occurs.

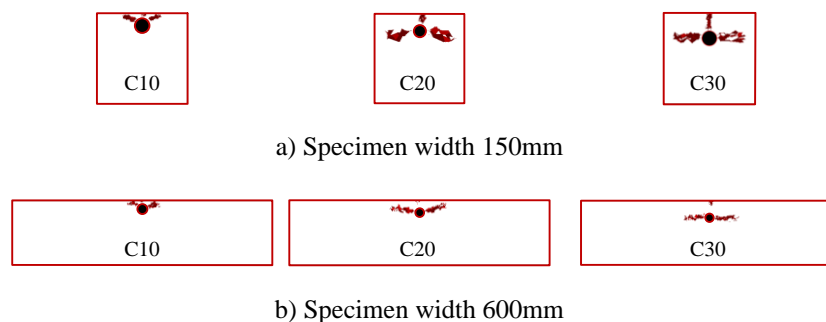


Figure 10: Internal crack patterns of normal concrete specimens

4. EFFECTS OF MATERIAL PROPERTIES ON CRACK DEVELOPMENT

4.1. Surface crack development

Figure 11 presents surface crack development for different tensile strengths. It is all shown that corrosion amount for surface crack initiation increases with tensile strength. However surface crack width develops following nearly the same route after initiation. Although surface crack generation is delayed by high tensile strength, a bigger crack opening will appear conversely and then expand quickly. It can be deduced that surface crack propagation is not related with tensile strength.

Figure 12 displays surface crack propagation for different fracture energies. The same tendency is shown in concrete specimens with different geometrical properties, i.e. surface crack width decrease obviously when fracture energy increases. Compared with impacts of tensile strength, it seems that surface crack propagation is controlled by fracture energy while tensile strength is dominant in crack initiation. Hence, ductile materials with high fracture energies can be used to control surface crack development for maintenance of cracked concrete due to rebar corrosion.

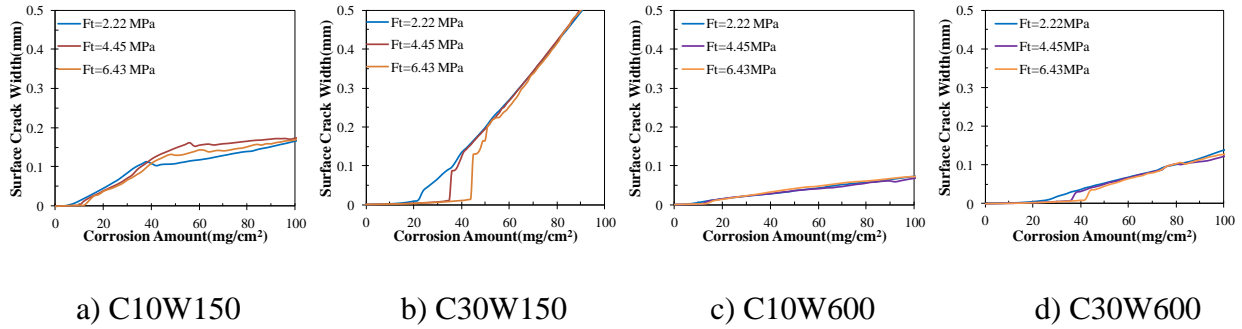


Figure 11: Surface crack development for different tensile strengths

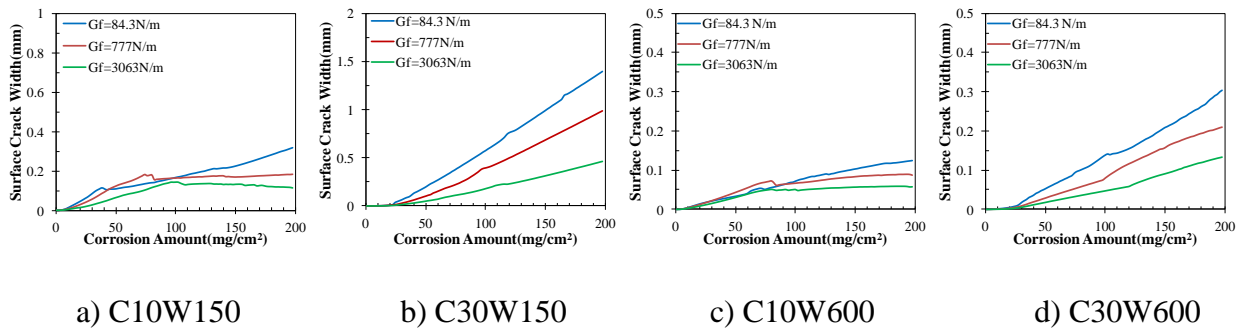


Figure 12: Surface crack development for different fracture energies

4.2. Internal crack propagation

Internal crack pattern is highly related with fracture energy for wide concrete specimens. Figure 13 depicts internal crack pattern corresponding to corrosion amount of 70mg/cm², 100mg/cm² and 140 mg/cm² separately for specimen width of 150mm. In this case, different fracture energies result in the same crack pattern, i.e. lateral cracks develop toward sides of specimen along with vertical crack propagating from surface to rebar. The effect of fracture energy is merely that crack propagation becomes slow.

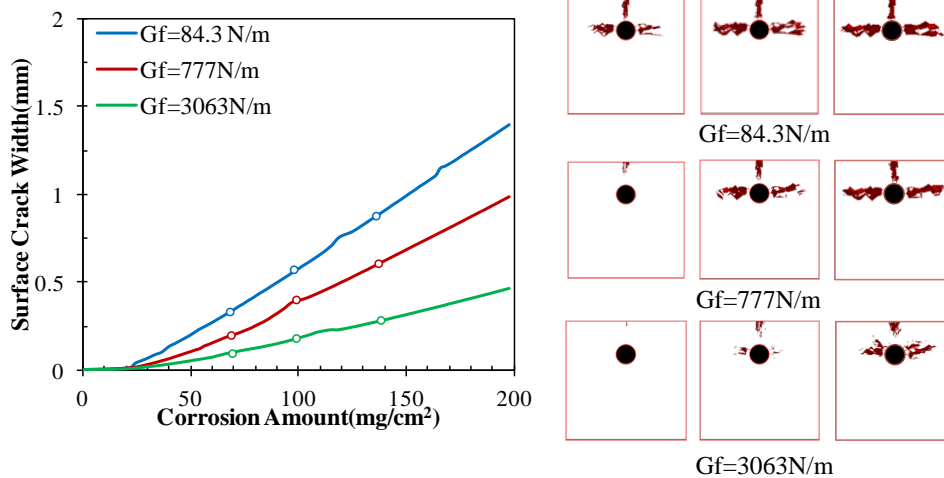


Figure 13: Internal crack pattern for specimen with a width of 150mm

Figure 14 presents internal crack pattern of specimen with a width of 600mm under the corrosion amount of 100, 140 and 170 mg/cm^2 separately. It can be found that high fracture energy leads to lateral cracks developing diagonally toward concrete surface. Besides, lateral crack length decreases evidently with an increase of fracture energy. It is identified that ductile materials with high fracture energy used in repair will limit cracked area and hence reduce spalling area of reinforced concrete.

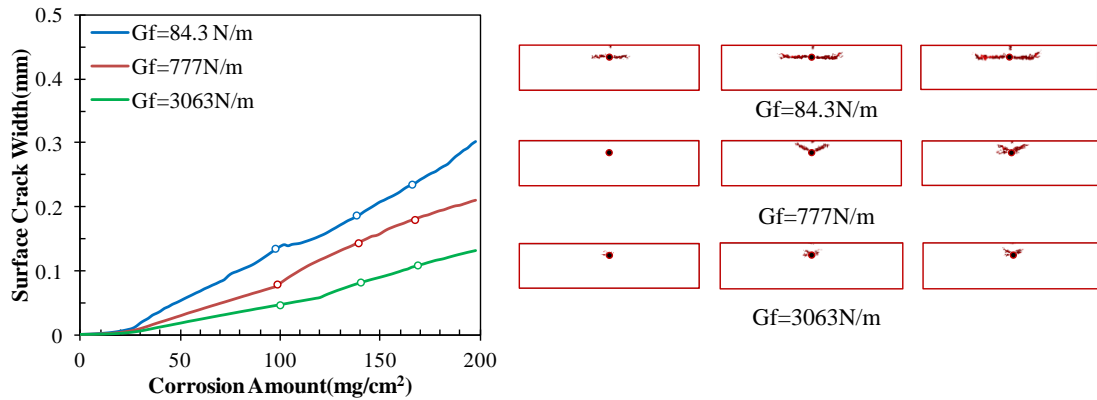


Figure 14: Internal crack pattern for specimen with a width of 600mm

5. CONCLUSIONS

Generally, it can be concluded from the simulation work that:

- 1) For normal concrete, a wider specimen or thicker cover will result in smaller surface crack width. Decreasing cover thickness will cause an early crack initiation and internal cracks propagate to concrete surface.
- 2) Surface crack initiation is determined by tensile strength while fracture energy renders a big influence on surface crack evolution.
- 3) Increasing fracture energy for wide specimen will cause internal cracks propagate toward concrete surface and reduce the spalling volume of concrete cover.
- 4) Utilization of ductile materials with high fracture energy will be beneficial to control surface crack width and also to confine spalling area of concrete slab in danger of rebar corrosion.

REFERENCES

- Alonso C, Andrade C, Rodriguez J and Diez JM (1998). Factors Controlling Cracking of Concrete affected by Reinforcement Corrosion, *Materials and Structures*, 31, pp. 435-441.
- Tran KK, Nakamura H, Kawamura K and Kunieda M (2011). Analysis of Crack Propagation due to Rebar Corrosion using RBSM, *Cement and Concrete Composites*, 33(9), pp. 906-917.
- Tsutsumi T, Matsushima M, Murakami Y and Seki H (1996). Study on Crack Models caused by Pressure due to Corrosion Products, *Doboku Gakkai Ronbunshuu*, 30(2), pp. 159-166 (in Japanese).
- Xiao PW, Yi N, Su LW, Li GB and Wang LB (2011). Finite Element Analysis of Expansive Behaviour due to Reinforced Corrosion in RC Structure, *Procedia Engineering*, 12, pp. 117-126.
- Yamamoto Y, Nakamura H, Kuroda I, and Furuya N (2008). Analysis of Compression Failure of Concrete by Three Dimensional Rigid Body Spring Model. *Doboku Gakkai Ronbunshuu*. 64(4), pp.612-630 (in Japanese).